EXPERIMENTAL AND NUMERICAL STUDY ON BUCKLING OF AXIALLY COMPRESSED COMPOSITE CYLINDERS

CENTRISKI SPIESTU KOMPOZĪTO CILINDRU NOTURĪBAS EKSPERIMENTĀLS UN SKAITLISKS PĒTĪJUMS

E. Eglītis, K. Kalniņš, O. Ozoliņš

Keywords: buckling, imperfecitons, axially compressed cylinders, composite shells, buckling experiments

1. Introduction

Thin shells are efficient structures that can support very high buckling loads. However, unlike columns and plates, shells usually have a very unstable post-buckling behaviour that strongly influences their buckling characteristics. Hence their buckling and post-buckling have presented scientific and engineering challenges for decades. [1] Axially compressed cylinder may be one of the last classical problems in structural mechanics for which it remains difficult to obtain close agreement between careful experiments and the best predictions from numerical modelling, therefore this is a subject of continuous research. [2]

Buckling and post-buckling of axially compressed, homogenous isotropic cylinders has been investigated since it was first identified in the beginning of the last century by “wrinkling” or “secondary flexure” in columns. [3] In practice, buckling of cylindrical shells under axial compression became important as their use in aircraft structures broadened as thin-walled columns and stressed-skin construction of fuselages and wings, introduced in the late twenties. Since then the shell buckling phenomena became the central design problem of aerospace structures. [4]

According to the well-known and accepted linear classical theory, the linear bifurcation buckling stress for a perfect isotropic cylindrical shell under ideal conditions (of medium length, with pre-buckling stresses by the boundary conditions and boundaries that restrain circumferential displacements during buckling) is (1):

$$\sigma_{cr} = \frac{E}{\sqrt{3(1-\nu^2)}}\frac{t}{r}, \qquad (1)$$

where E is the elastic modulus of the material, ν is the Poisson ratio, t is wall thickness and r is the radius of the cylinder. This buckling stress equation was independently found by Lorenz [5], Timoshenko [6] and Southwell [7] and is known as the “classical elastic critical stress”.

At this buckling stress, a very large number of different buckling modes or eigenmodes are all simultaneously critical, sometimes over 100 modes within 1% above the first one. The steeply falling post-buckling path is associated with the proximity of these many modes. [2]

As mentioned before, significant effort has been applied to understand the post-buckling phenomena for axially compressed cylinders, though it is still difficult to obtain good accordance of experimental results and numerical predictions. The initial imperfections are dependant on production technology and post-processing, therefore it is still impossible to produce cylinders with no imperfections that would affect the buckling strength. There are imperfections in the shell geometry, thickness variations, residual stresses and poor definition of boundary conditions. It is widely accepted that the most important factor contributing to the discrepancy between theory and experiment for axially compressed cylinders is initial imperfections in the shell geometry. [2, 8] Since initial imperfections are obviously random by nature, stochastic stability analysis can be used. The buckling of imperfection sensitive structures with small random imperfections has been studied by several investigators, such as Bolotin [9], Faser and Budiansky [10] and Amazigo [11]. However, considering

the absence of experimental evidence about type of imperfections that occur in practice and in order to reduce the mathematical complexity of the problem, all the above-named investigators have been working with some form of idealised imperfection distribution. [1]
Extensive experimental and analytical studies on the buckling of composite cylinders made of carbon fibre reinforced plastics (CFRP) have been conducted at the Institute for Aerospace Studies, University of Toronto in the seventies and eighties. Special emphasis was given in these studies to the effect of initial geometrical imperfections of the cylinder. The random distributions of the geometrical imperfections of the shells were determined by mounting the shell in a transversing device equipped with two, diametrically opposed low pressure, linear contracting transducers. The imperfection data was fed into Fourier analysis program, and imperfection amplitudes and an estimated line of power spectral density as a function of special frequency was computed. The data recorded by transducers were also used to compute the average shell thickness. The cylinders were tested with their ends clamped into fitted aluminium plates and bonded.
The analytical estimates of the buckling capacity of the imperfect shells were based on the maximum value of the imperfection amplitude, which was obtained from the statistical representation of the measured initial geometrical imperfection. The magnitude of the imperfection amplitude was in the order of the shell wall thickness, and resulted in significantly lower buckling strength comparing to perfect cylinders. It has been reported that the agreement between the predicted response and the experiments was consistently good, with discrepancy not exceeding 20 percent. [12]
More recently, buckling tests on composite cylinders manufactured from CFRP prepregnated material were conducted at the German Aerospace centre DLR, Brauschweig, Germany. One study was devoted to experimental confirmation of the computed large difference between the optimum and pessimum designs, where the optimum may be as high as 2.8 times that of the worst one, for laminates consisting of the same number of plies. The comparison with the analytical predictions yielded in “knock-down” factors ranging from 0.80 – 1.03, their scatter was small and they were not significantly smaller for the optimal cylinders (about 0.8) than the pessimal ones (about 0.9). [13]
The same authors also have performed search for imperfection tolerant laminate lay-up. The results show that imperfection sensitivity of composite cylinders depends on lay up. A knock-down factor of 0.68 was experienced with the (±75/±75) laminates, while a knock-down factor of 0.91 was found for the (0_2/±19/±37/±45/±51) laminates. [14]
Extensive experimental, analytical and numerical investigations on the buckling behaviour of composite cylindrical shells were carried out at the Departments of Aerospace Engineering and Structural Engineering, Politechnico di Milano, Italy. The cylinders investigated were 700 mm long, with 700 mm diameter and reinforced at the ends to facilitate their fixing into loading rig. Cross-ply $(0/90)_S$, angle-ply $(\pm 45)_S$ and eight-ply quasi-isotropic lay-ups were used in these investigations. Particular attention has been paid to the boundary conditions. The employed loading rig provided good-accuracy displacement-controlled loading, and elaborate clamping devices were used to constrain the ends of the specimens. The inner and outer surfaces were scanned using non-contact measuring device to record the initial geometrical imperfections and their growth during the loading. The results were compared to theoretical predictions and knock-down factors raging from 0.86 for angle-ply cylinders to 0.88 for cross-ply cylinders were obtained. [15]
There are are number of studies performed on post-buckling of composite cylinders, which included measuring of initial imperfections and applying to numerical models. These investigations include works by Meyer-Piening et al. [16] and Bisagni et al. [17]. Employing the updated models, fair agreement of experimental and numerical results has been achieved for torsional loading.
Most investigations on buckling of axially compressed cylinders have been focused on metallic cylindrical shells. In this paper, buckling behaviour of thin E-glass fabric/polyester resin matrix composite cylinders of medium length has been investigated.

2. Specimens

Series of thin cylinders have been produced for this study. All the specimens share the same wall thickness of 1.1 mm and material – E-glass fibre fabric / polyester resin matrix composite. 290 g/m^2

fabric was used and 4 layers of fabric were winded to achieve the specified wall thickness. The cylinders had diameters (*D*) of 300 mm and 500 mm and lengths (L) of 400 mm, 560 mm and 660 mm. Numbers of the specimens and their dimensions are presented in Table 1. Additionally, flat specimens of the same fabric and resin were produced for determination of material properties according to LVS EN ISO 527-4:2000 [18] standard.

Table 1

Dimensions and designations of specimens

<table>
<tr><th colspan="2" rowspan="2"></th><th colspan="2">Diameter D</th></tr>
<tr><th>300 mm</th><th>500 mm</th></tr>
<tr><th rowspan="3">Free length L</th><th>400 mm</th><td>RTU #6
RTU #12
RTU #13
RTU #16</td><td>-</td></tr>
<tr><th>560 mm</th><td>RTU #3
RTU #4
RTU #5
RTU #7</td><td>-</td></tr>
<tr><th>660 mm</th><td>RTU #9
RTU #10
RTU #11</td><td>RTU #1-1
RTU #1-2
RTU #1-3
RTU #1-4
RTU #1-5
RTU #1-6
RTU #1-7</td></tr>
</table>

All the specimens were produced employing cylindrical, slightly conical mould. The conical shape is necessary for easy removal of the specimens without any damage. Vacuum bag moulding was employed to remove excess resin and ensure more consistent material properties, excluding specimens RTU #1-5 through RTU #1-7. The flat specimens were produced using vacuum bag moulding as well.

The specimens with diameter of 300 mm were cured in an autoclave with 80˚C temperature, but specimens with diameter of 500 mm were cured in ambient temperature of about 20˚C.

Special end fixture was necessary [19] to assure balanced load distribution and consistent boundary conditions (see Fig. 1). After curing the specimens were cut to their lengths and the ends were potted into gaps of circular plates using mixture of aluminium powder and epoxy resin. The plates were cut out of MDF and plywood boards for specimens of 500 mm and 300 mm in diameter, respectively.

Finally, the specimens were painted white using acrylic spray paint for post-buckling shape monitoring using moiré fringes.

3. Determination of material properties

The material properties have been determined by tensile experiments, where the flat plates were cut into tension specimens. The tests were performed according to the ISO 527-4:2000 standard, and the chosen specimen configuration is shown in Fig. 2. According to the standard, end tabs were bonded before cutting. Tensile tests were performed at a laboratory of the RTU Institute of Materials and Structures, equipped with Zwick Z100 machine. The test was displacement-controlled, the load was measured by a load cell and the strains were registered by a laser extensometer. Total of 14 specimens were tested, half of them in 0º direction and other half in 90º direction. The average elastic modulus was computed for every direction separately from the 0.05% to 0.25% strain, according to the ISO standard. The obtained load-extension curves are presented on Fig. 3.

The average elastic modulus *E* of this E-glass fibre fabric / polyester resin matrix composite has been measured 18.28 GPa in 0º direction and 18.66 GPa in 90º direction and the standard deviations are

0.78 MPa and 0.48 MPa, respectively. The average measured breaking tensile stress σ_{max} was registered 219 MPa with 13 MPa standard deviation in 0º direction and 296 MPa in 90º direction with 26 MPa standard deviation.

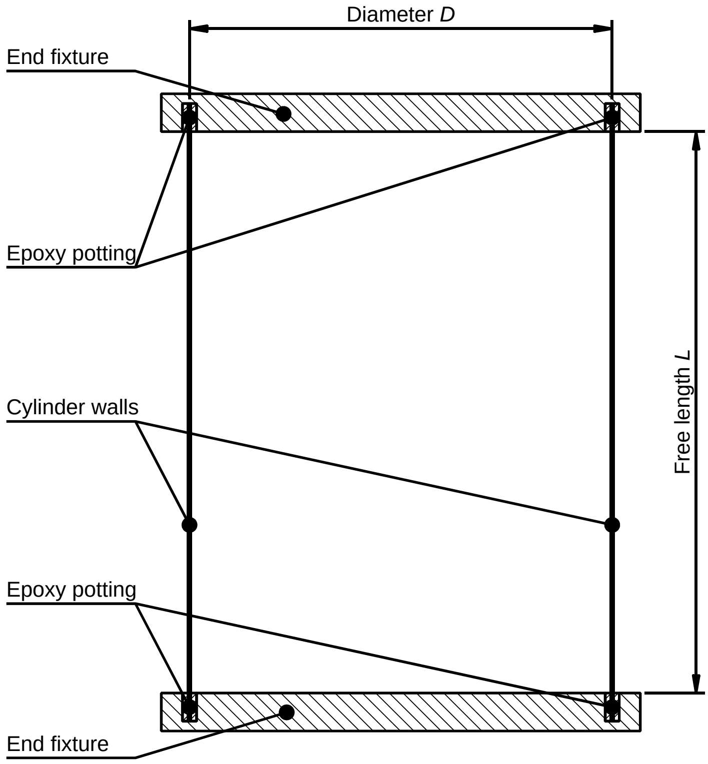

Fig. 1
The test specimen

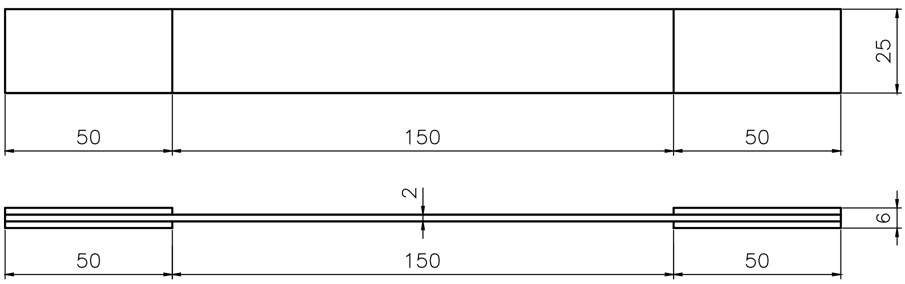

Fig. 2
Specimen for determination of composite's tensile properties

4. Experimental set-up

The experimental rig prepared at the laboratory of the RTU Institute of Materials and Structures consists of Instron 8802 hydraulic frame, Instron 3520 hydraulic pump, Instron 8800 Fast Track controller and a computer (Fig. 4). The load is being introduced through pair of grips and two steel plates. The top plate is fixed to the grip, while the bottom plate is spherically supported to distribute the load evenly when the specimen end plates aren't strictly parallel. The rotation centre of the spherical support is 150 mm above the bottom plate. The load cell that registers the axial load of the cylinder is located between the lower grip and the frame.

In order to monitor the post-buckling shapes of the cylinders, a basic interferometry set-up has been created. A moiré fringe with both line thickness and distance between lines of 1 mm was placed in front of the specimens. Placing a spotlight and a camera at different angles resulted in pictures with moiré patterns clearly indicating post-buckling shapes on the taken pictures (Fig.7, 8).

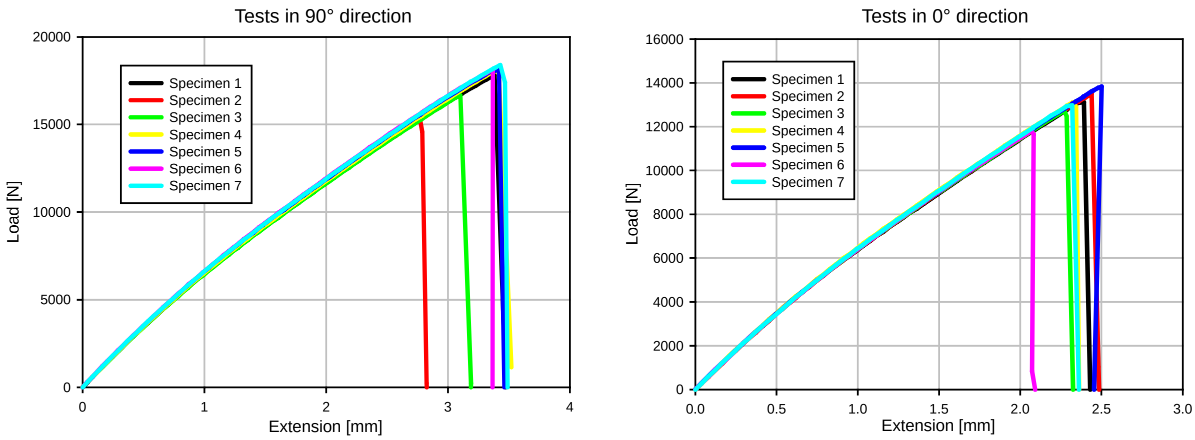

Fig. 3
Load-extension curves of the tests for determination of tensile properties

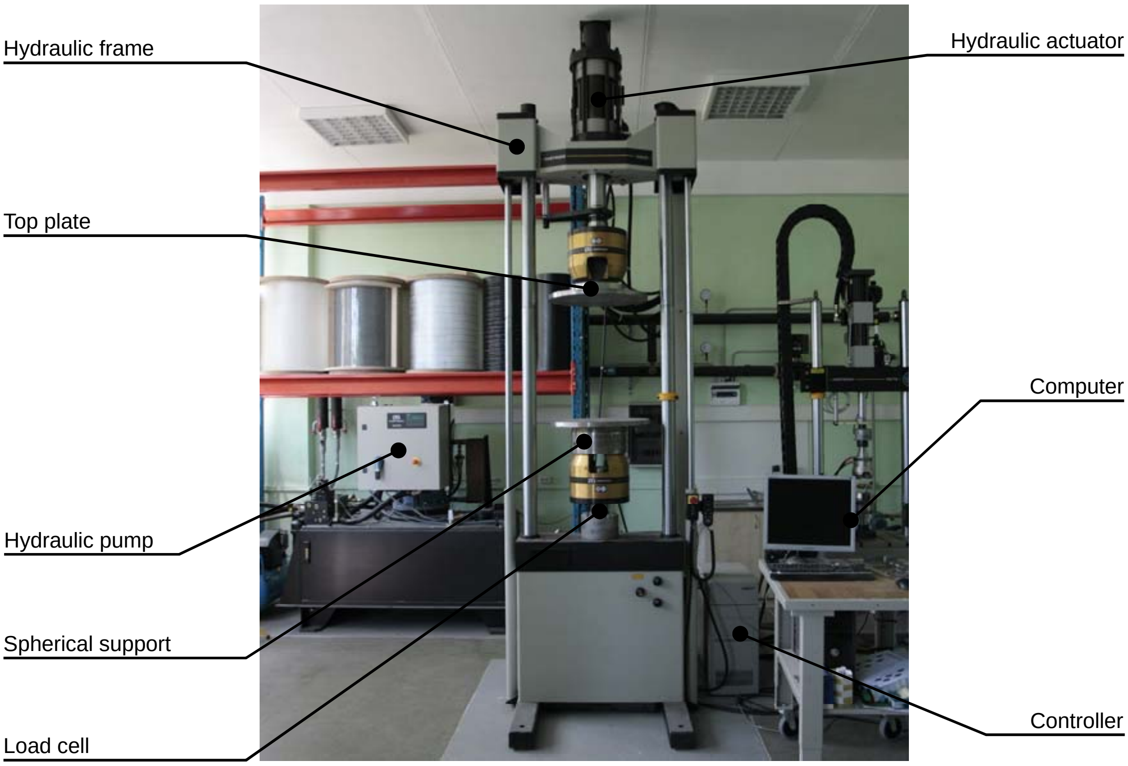

Fig. 4
The set-up for buckling experiments

5. Experimental results

All the specimens were repeatedly loaded until post-buckling to determine their buckling loads and corresponding buckling shapes within a timeframe of 6 months. The scatters of obtained critical load values for specimens with diameters of 300 mm and 500 mm are summarized in Figure 5 and Figure 6, respectively. It should be noted that the results for specimens with different lengths are presented on the same figure, as according to the linear classical theory the buckling load for a perfect cylindrical shell is not dependent on it's length, as the shells under investigation are of medium length [2].

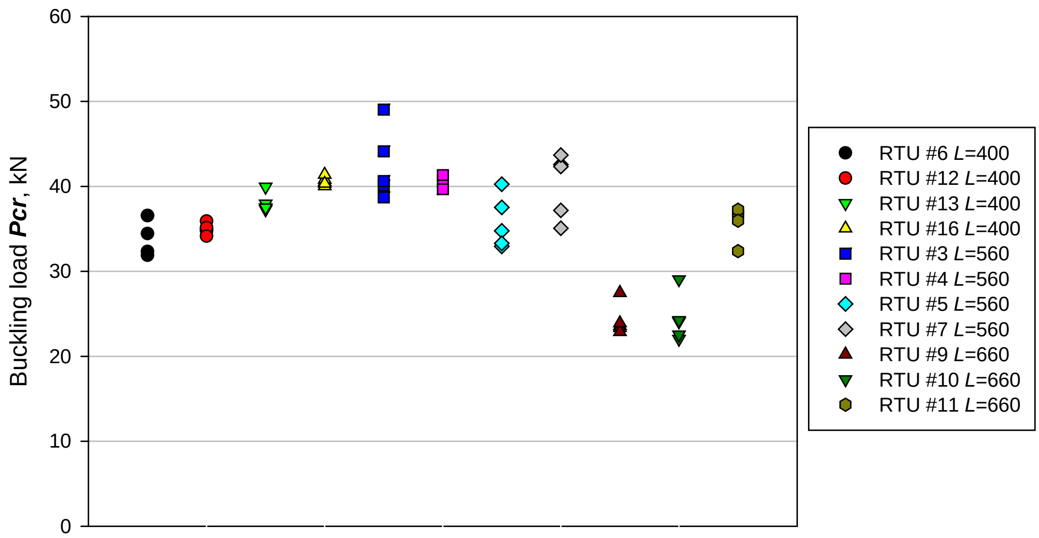

Fig. 5
Buckling loads for D = 300 mm specimens

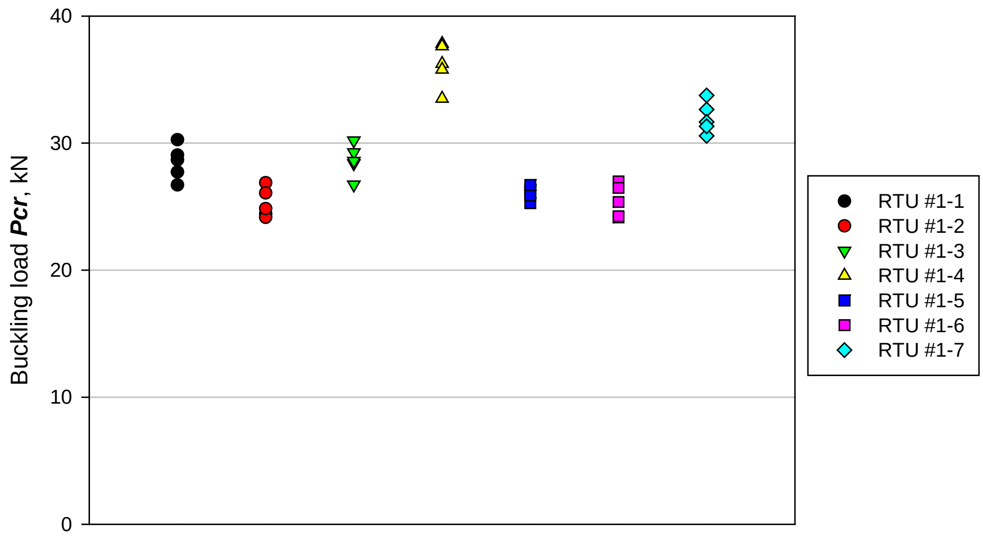

Fig. 6
Buckling loads for D = 500 mm specimens

As it is seen from the scatter plots, there is significant discrepancy between the maximum and minimum buckling loads. Comparing all the results for the cylinders of the same diameter, the observed difference is 60% for 300 mm specimens and 40% for 500 mm specimens. The differences are significantly smaller when comparing only the results for each cylinder. Average experimentally obtained buckling loads and their standard deviations for each cylinder configuration are summarized in Table 3.
For some cylinders the buckling loads had a minor scatter during the repeated loading, as for cylinders RTU #1-5, RTU #7, RTU #12, RTU #13, RTU #16. However, for some cylinders, the buckling load and also post-buckling behaviour did vary significantly, as in case of cylinders RTU #3, RTU #5 and RTU #7. However, no visible damage has been observed on these specimens.

Not only the buckling loads differ, but the registered post-buckling mode shapes of the cylinders as well. Pictures of the typical post-buckling mode shapes for the 300 mm and 500 mm cylinders are summarized in Figures 7 and 8. The load-shortening curves with the maximum and minimum obtained buckling loads for each specimen configuration are presented in Figure 9.

After performing the ABAQUS/Explicit [20] finite element analysis and obtaining the buckling modes, it is clearly evident that the specimens having the buckling modes close to the numerically obtained have the highest buckling loads. The specimen with the highest load-carrying capacity for each configuration, namely, RTU #1-4, RTU #3, RTU #11 and RTU #16 all have fairly similar buckling mode shapes (see Figures 7 and 8) comparing to the buckling mode shapes obtained numerically (see Figure 15). It should be also noted that the pre-buckling stiffness, recorded during the experiments, is significantly lower than the calculated one in case of D = 500 mm specimens. It can be explained by the low elastic modulus of the MDF end fixture used for these specimens and the fact that the shortening has been measured between the steel loading plates.

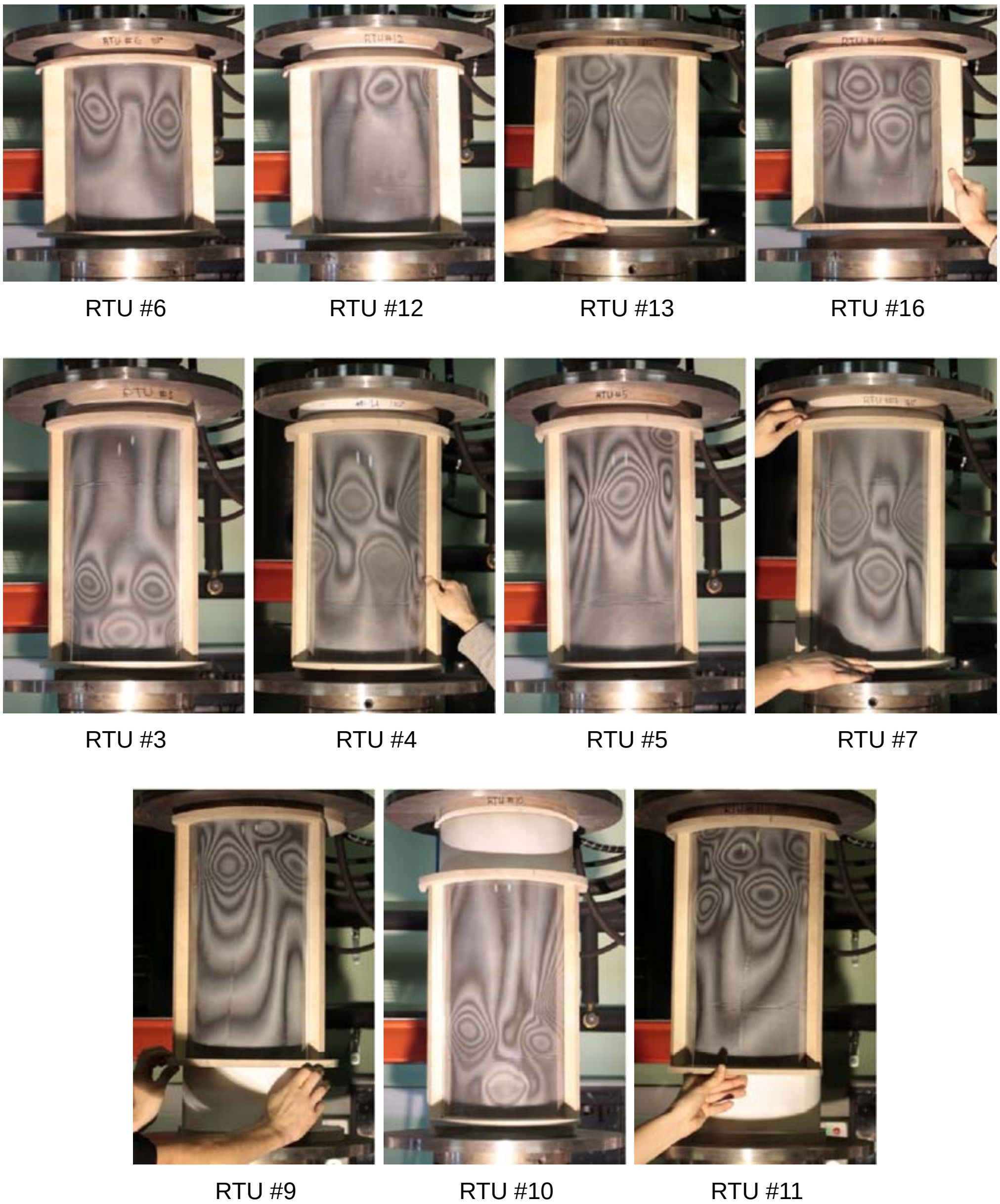

Fig. 7

Experimentally obtained buckling mode shapes of D = 300 mm specimens

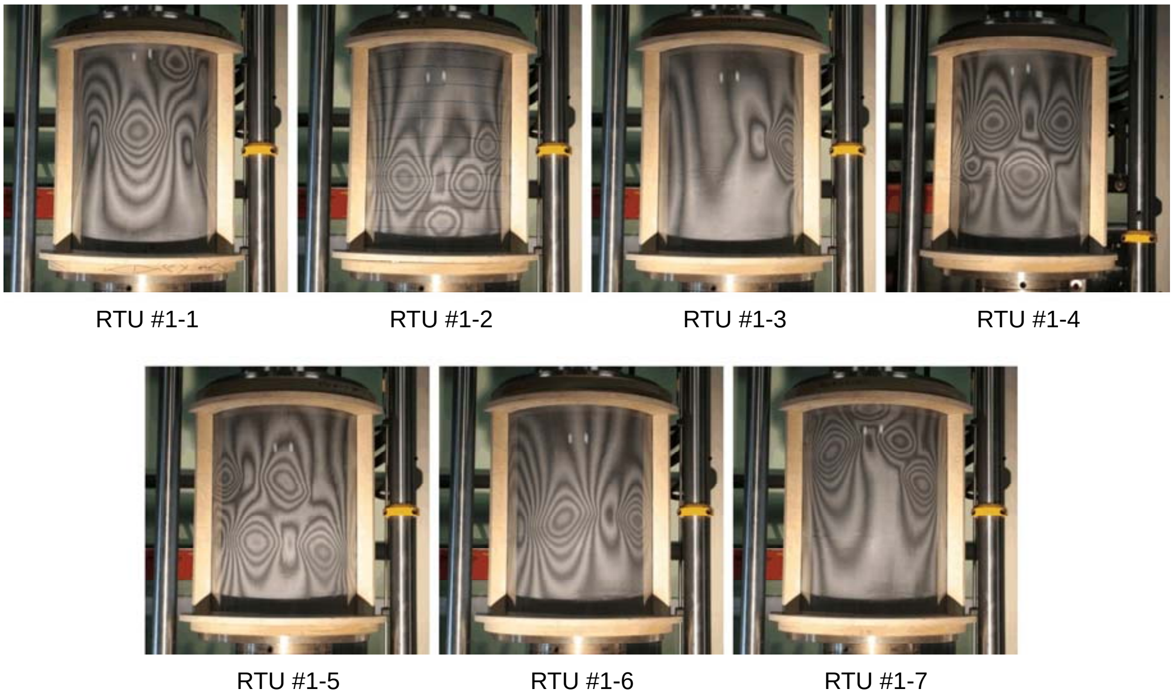

Fig. 8
Experimentally obtained buckling mode shapes of D = 500 mm specimens

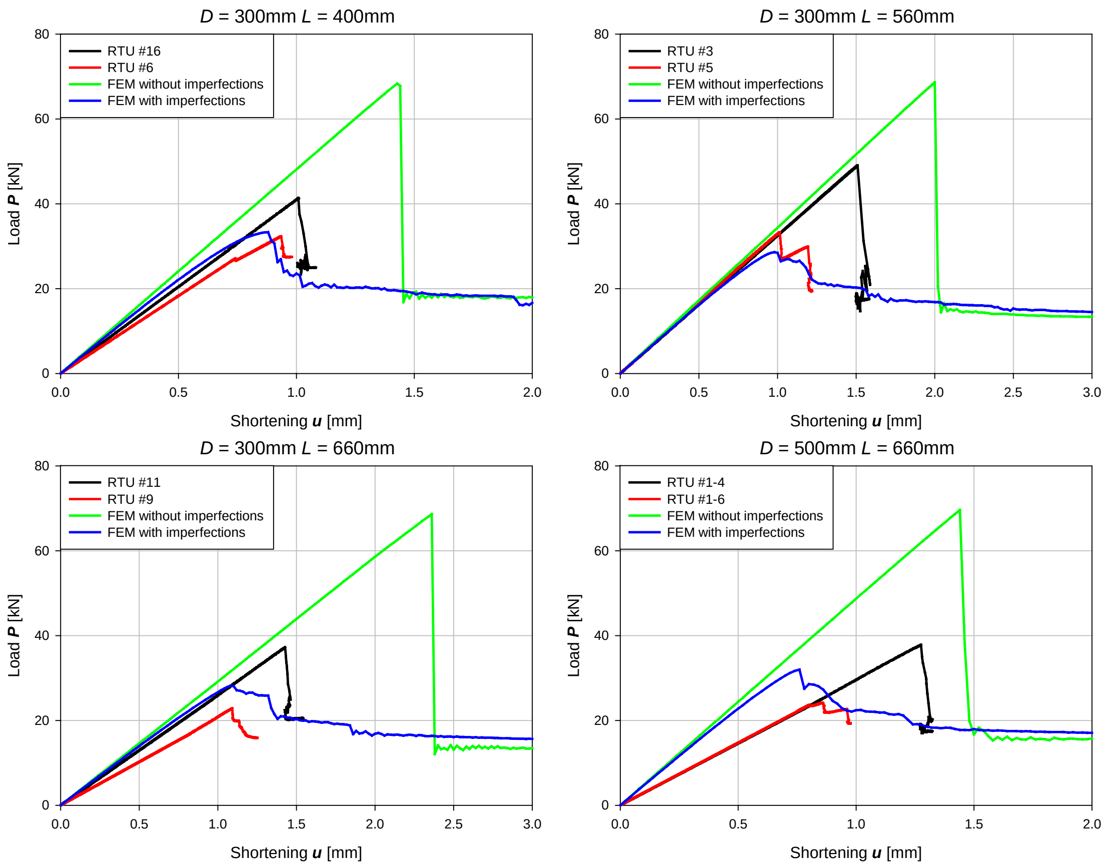

Fig. 9
Load-shortening curves for experiments where maximum and minimum buckling loads have been obtained for each configuration, and results of ABAQUS/Explicit numerical analysis

6. Finite Element modelling

Finite Element models of the experimentally investigated shells have been created to assess the accordance with numerically obtained result. ANSYS [21] and ABAQUS/Implicit [20] finite element codes were considered for this task. The results of linear analysis are buckling modes that are very far from the experimentally obtained ones (compare Fig. 10 *a*, *b* and Fig.7, Fig. 8), thus confirming that the linear eigenvalue and eigenmode analysis techniques can't be used for comparison with physical tests. However, linear analysis was used later for calculation of eigenmodes that were applied to the model as "worst case scenario" imperfections. The effect of these artificial geometrical imperfections will be discussed later in this article. In case of non-linear analysis, implicit finite element codes had serious convergence problems and therefore very unrealistic initial imperfections or too high damping factors had to be applied to obtain converging solution. Thus, ABAQUS/Explicit dynamic solution has been used to perform the non-linear buckling analysis throughout the study [20].

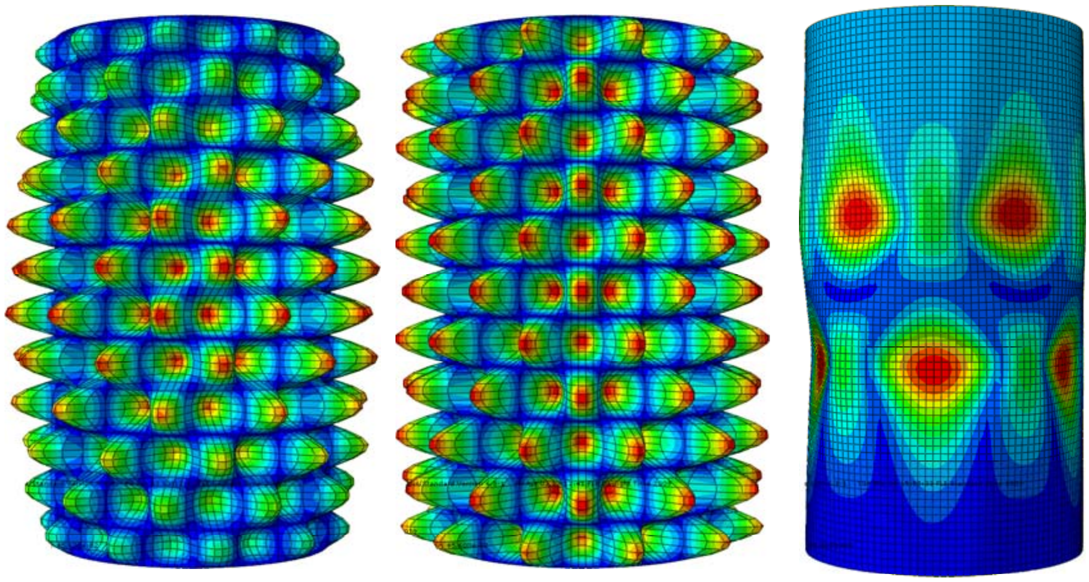

a *b* *c*

Fig. 10

Eigenmodes and Post-buckling mode shapes of 300 mm cylinders: *a* – first eigenmode (Pcr=69.9 kN); *b* – 50th eigenmode (Pcr=72.5 kN); *c* – non-linear post-buckling mode (Pcr=68.6 kN)

The study on mesh sensitivity and boundary condition study has been performed to elaborate a suitable modelling approach. According to the benchmark results presented in [22] 4-node shell element S4R has been selected. The mesh sensitivity analysis results show that element size to shell radius ratio of 1/20 is most appropriate for the simulation. The load-shortening curves obtained during the mesh sensitivity analysis are presented in Fig. 11*a* and the corresponding post-buckling mode shapes are summarized in Fig. 12. The mesh sensitivity analysis was performed on two model sizes – on D = 300 mm and L = 560 mm model, and on D = 500 mm diameter and L = 660 mm model. Simply supported boundary conditions were used throughout the mesh sensitivity analysis.
Three sets of boundary conditions were considered during this study (see Fig. 13) – simply supported (SS) and clamped along the edges (CL), and a set designated as (SF). The latter is a boundary condition set for more realistic representation of the conditions during the experiment that incorporates a rigid body connecting the lower edge of the specimen with a reference point located at the centre of the spherical support. The difference between the predicted buckling loads in the cases of simply supported and clamped boundary conditions did not exceed 5% and therefore the less constraining simply supported boundary conditions were used for the idealized reference model. The SF boundary conditions included 10 mm eccentricity of the reference point, which represents the random

eccentricity that can occur during the physical test. This modelling approach resulted in buckling mode shapes covering only one side of the circumference (see Fig. 14), as observed during the experiments, and slightly lower buckling loads. The load-shortening curves for the three boundary condition sets are presented in Fig. 11*b*. It is evident that inclusion of loading eccentricity of 10 mm affects the model with smaller radius more than the model with greater radius.

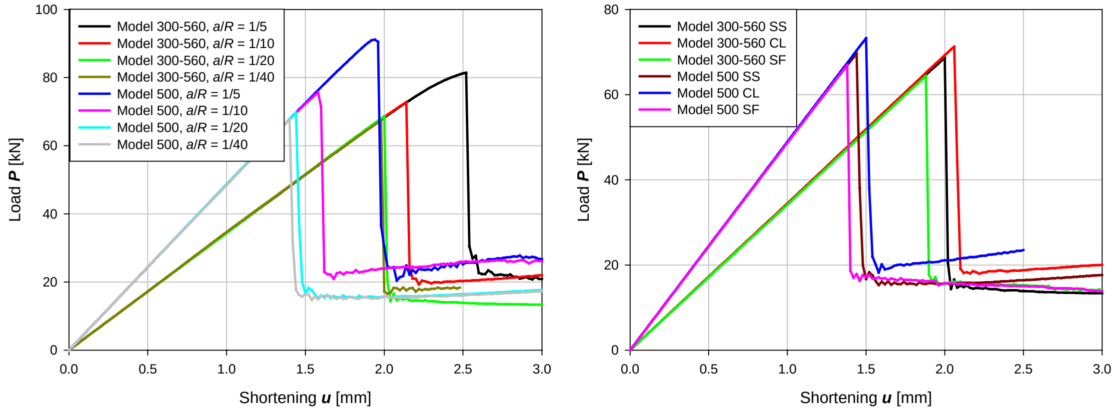

a *b*

Fig. 11

a - Results of the mesh sensitivity analysis.

b - Load-shortening curves obtained with different boundary condition sets: SS – simply supported, CL – clamped, SF – with simulation of spherical support

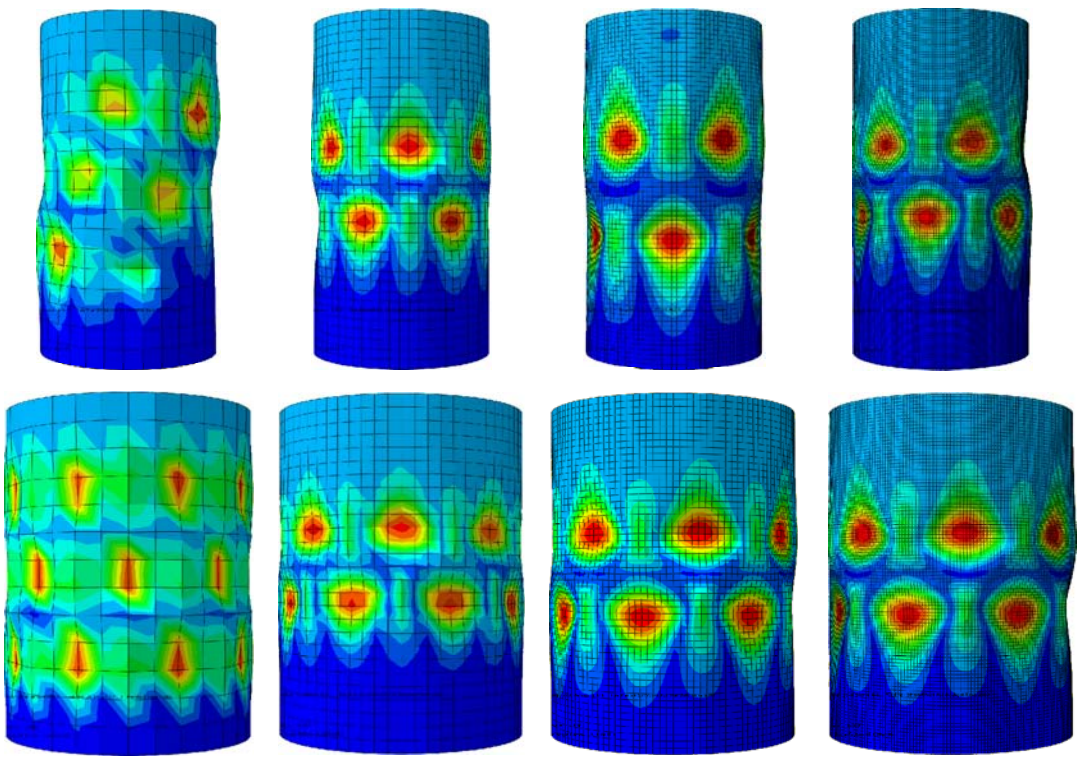

a/*R*=1/5 *a*/*R*=1/10 *a*/*R*=1/20 *a*/*R*=1/40

Fig. 12

Buckling modes obtained during the mesh sensitivity analysis for D = 300 mm and D = 500 mm

The SF boundary conditions were used to perform the imperfection sensitivity analysis. Eigenmodes were calculated for all of the specimens, and their shapes were used to introduce geometrical imperfections. As the eigenvalues are very closely spaced, one of the first 10 eigenmodes was chosen for introduction of the imperfections, so the buckling pattern would cover largest part of the shell. Imperfection amplitudes were 1/1, 1/2, 1/4 and 1/8 of the skin thickness. The results of imperfection sensitivity analysis will be discussed in the next chapter.

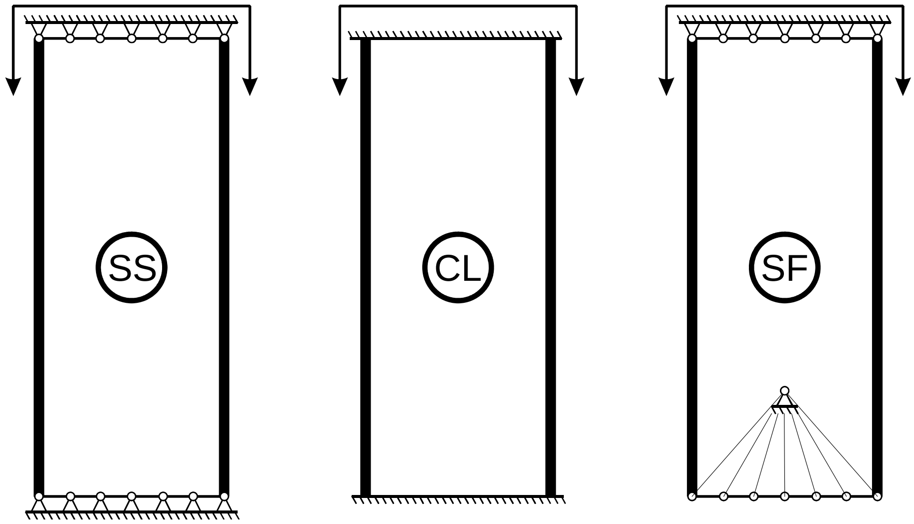

Fig. 13
Boundary condition sets considered for numerical analysis

7. Numerical results

According to the linear theory, the critical stress of perfect, anisotropic cylindrical shell is

$$\sigma_{cr} = \frac{E_1}{\sqrt{3(1-\nu_1\nu_2)}}\sqrt{\frac{E_2}{E_1}}\frac{t}{r}. \text{ [23]} \qquad (2)$$

As the elastic moduli E_1 and E_2, and ν_1 and ν_2 are very close for the material under investigation, equation (2) becomes the same as the one for isotropic shells (1). According to this formula, the critical stress for a perfect axially compressed cylindrical shell is not dependent on its length. After modifying the formula to calculate the critical load, the shell radius parameter is also absent:

$$P_{cr} = 2\pi r t \sigma_{cr} = 2\pi t^2 \frac{E}{\sqrt{3(1-\nu^2)}}, \qquad (3)$$

and thus the buckling load is not dependent on the shell radius as well. As the wall thickness of all of the specimens investigated was constant, the critical buckling load of perfect shells for all of the specimen sizes is equal to 84.09 kN.
The critical loads obtained from non-linear buckling analysis for the idealized models (with simply supported boundary conditions and no imperfections) and "realistic models" with different factors of initial imperfections are summarized in Table 2. The corresponding load-shortening curves are presented in Fig. 15.
The results for the idealized models with simply supported boundary conditions confirm the small influence of the length of the cylinder on the buckling load. Comparison of the results for models with

different radius shows the small influence of the radius as well. All the differences are within 5% for the models with simply supported boundary conditions.

Table 2

Critical loads for the models considered

	Model 300-400	Model 300-560	Model 300-660	Model 500-660
Analytical formula	84.09 kN	84.09 kN	84.09 kN	84.09 kN
SS, no imperfections	68.36 kN	68.64 kN	68.64 kN	69.62 kN
SF, no imperfections	63.14 kN	64.36 kN	64.52 kN	66.94 kN
SF, imperfection factor *t*/8	44.39 kN	44.99 kN	45.27 kN	48.46 kN
SF, imperfection factor *t*/4	37.09 kN	37.15 kN	36.90 kN	39.54 kN
SF, imperfection factor *t*/2	34.12 kN	31.82 kN	32.47 kN	34.80 kN
SF, imperfection factor *t*	33.31 kN	28.59 kN	28.18 kN	31.97 kN

It is also evident that buckling loads calculated with non-linear ABAQUS/Explicit finite element code are about 18% lower that the ones calculated using the analytical formula (2) based on linear classical theory.
The buckling modes obtained with the non-linear numerical analysis are in good agreement with the experiments, considering the fact that the initial geometrical imperfections of the experimentally investigated specimens were not included in the analysis. The tested specimens that have the greatest critical buckling loads and therefore least initial imperfections had buckling patterns very similar to the modes obtained by the "realistic" model that included the spherical support (see Fig. 14). The buckling modes for idealized model with simply supported boundary conditions were similar, except the buckles were of same magnitude all across the circumference.
Updating the model with representation of the spherical support also resulted in drop of numerically obtained critical buckling load by more than 10%. This makes the numerical solution closer to the experimental results, however, the ABAQUS finite element predictions still give a considerable overestimation of the buckling load comparing to the experiments.

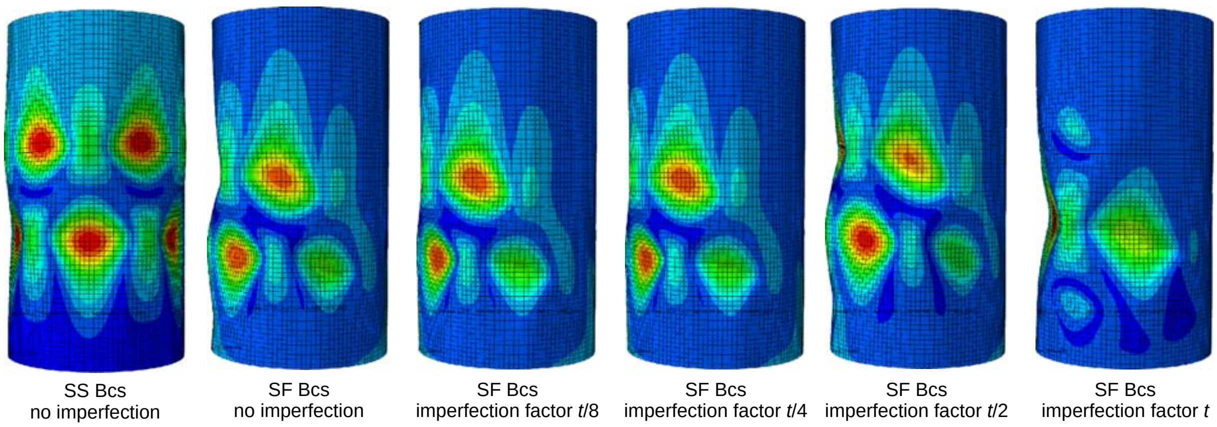

Fig. 14

Influence of boundary conditions and magnitude of initial imperfections on post-buckling shape of the cylinder (results shown only for model 300-560)

Adding initial imperfections to the model decreases the numerically obtained buckling loads and confirms that the drop of the critical load depends on the shape and the magnitude of the imperfections. As the initial imperfections of the test specimens could not be measured, eigenmode shaped initial geometrical imperfections were applied to the finite element models. The magnitude of the imperfections is defined as the maximum deviation from the perfect geometry and is called "imperfection factor" in this paper. Fractions of the shell thickness were used as the imperfection factors in this study. Imperfection factor of *t*/8 results in a 30 % drop comparing to the intact model, and drop up to 59 % has been observed with the imperfection factor equal to the skin thickness *t*. Critical loads obtained analytically, with idealized finite element models and models with different imperfection factors are summarized in Table 2, and the corresponding load-shortening curves are shown in the Figure 15. The numerical results closest to the average experimental results are summarized in the Table 3. The results show, that it probably possible to predict average buckling loads of series of composite cylinders, provided that statistical data of their imperfection character and magnitude is available. Though, further studies on buckling of imperfect shells are needed, along with experimental and numerical imperfection sensitivity analysis of axially compressed composite cylinders.

Table 3

Comparison of experimental and numerical results

Specimen configuration	**Average experimental P_{cr} [kN]**	**Standard deviation [kN]**	**Closest numerical P_{cr} [kN]**	**Imperfection factor**
300-400	36.99	2.84	37.09	$t/4$
300-560	39.73	3.90	37.15	$t/4$
300-660	28.15	6.00	28.18	t
500-660	28.87	3.93	31.97	t

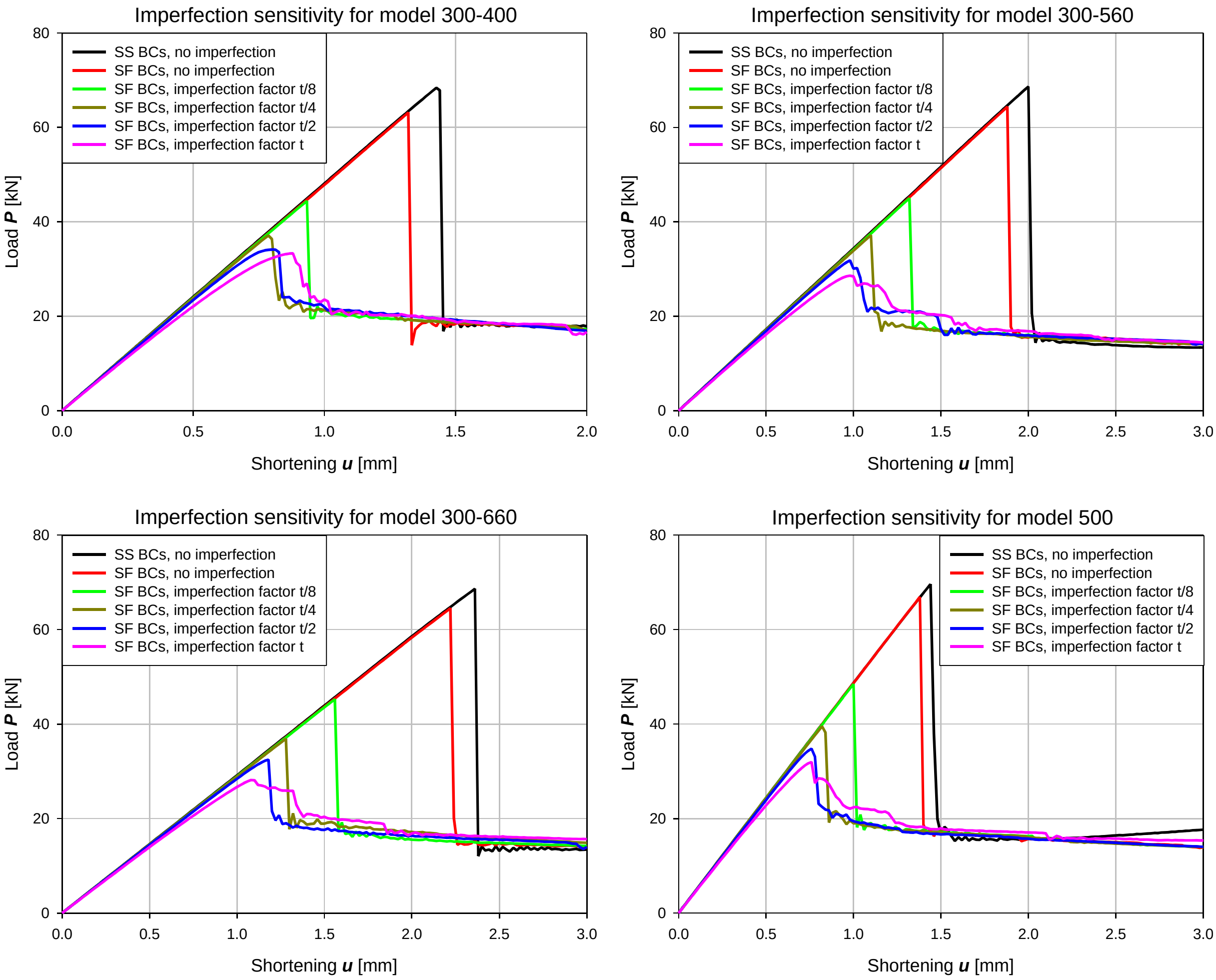

Fig. 15
Numerically obtained load-shortening curves for different imperfection magnitudes

8. Conclusions

An experimental and numerical investigation on buckling behaviour of composite cylinders has been performed. 18 specimens with diameters of 300 mm and 500 mm and lengths of 400 mm to 660 mm have been repeatedly loaded until post-buckling. The performed experiments were also simulated using ABAQUS/Explicit finite element code.
The experimental results had significant scatter of critical loads, differing up to 40% for the specimens that have same dimensions (see Figures 5 and 6), while the maximum difference between the results of repeated experiments was ranging from 3% in case of specimen RTU #16 to 21% in case of specimen RTU #3. The knockdown factors obtained in the experiments were ranging from 0.25 for specimen RTU #10 to 0.58 for specimen RTU #3. These knockdown factors are within the margins observed by Harris et al [24].
The numerical results have been obtained by ABAQUS/Explicit finite element code for perfect models of the test specimens as well as for models updated with more "realistic" boundary conditions and introduced initial imperfections. Use of ANSYS and ABAQUS/Implicit finite element codes has been assessed as well, but with less success due to highly non-linear response of the structure. The critical buckling loads were also analytically obtained using classical linear theory.
The comparison of experimentally obtained buckling mode shapes with the ones obtained by ABAQUS/Explicit show good accordance between the modes observed for the specimens with the highest buckling loads and the numerical result. However, the buckling loads of the perfect models are significantly higher than the highest experimentally obtained buckling loads, but lower than analytically obtained ones. Application of the artificial imperfections in shape of eigenmodes to the finite element model lowered the buckling load significantly and the higher magnitude imperfections also changed the numerically obtained buckling mode shapes. The shorter specimens have the greatest experimentally obtained buckling loads and least standard deviations in the test series, which means they have less initial imperfections. Consequently, relatively small imperfections had to be introduced to the numerical model to obtain close result. In contrary, the specimens with greater length had smaller buckling loads, greater standard deviations, and the greatest considered amplitude of artificial imperfections resulted in close numerical results.
Good agreement between experimental and numerical results can be observed, however, further studies are necessary. First of all, the effect of loading eccentricity has to be assessed to build a more realistic finite element model. Other materials and t/r ratios of specimens should be used to validate the results of finite element analysis. Technology for measurement of geometrical and thickness imperfections has to be developed to update the finite element models with actual imperfections. This measurement technology would also allow performing statistical analysis of imperfection size and shape of the imperfections in specimens, as well as quality control. A scanning technology that would allow measuring the buckled shape of the specimens should be developed for advanced comparison between experimental and numerical results. Some steps on adopting laser scanning equipment used in geomatics for these measurements have already been made.

Acknowledgement

This work has been partly supported by Latvian Council of Sciences through the project 09.1262 "Innovative design methodology for manufacturing of composite structures with physical validation" and by Riga Technical University through the project ZP-2008/3 "Scanning methods for quality control of three-dimensional composite structures"

References

1. Singer J., Arbocz J., Weller T. Buckling Experiments: Experimental Methods in Buckling of Thin-Walled Structures. - New York: John Wiley and Sons, Inc., 2004.
2. Teng J. G., Rotter J. M. Buckling of Thin Metal Shells. - London: Spon Press, 2004.
3. Lilly W. E. The Economic Design Of Columns // Transactions of Institution of Civil Engineers of Ireland (Dublin), March 1906, pp. 67-93.
4. Hoff N. J. Thin Shells in Aerospace Structures // Aeronautics and Astronautics, 5, February 1967, pp.26-45.
5. Lorenz R. Buckling of cylindrical shell shell under axial compression // Zeitschrift des Vereines Deutcher Ingenieure, 52, 1908, p. 1766.
6. Timoshenko S. P., Einige Stabilitätsprobleme der Elasticitätstheorie // Zeitschrift für Matematic und Physik, 58, 1910, pp.378-385.
7. Southwell R.V. // Philosophical Transactions of the Royal Society, 213, 1914, p. 187.
8. Eglītis E., Kalniņš K., Ozoliņš O., Rikards R. Numerical Study of Geometrical Imperfection Response on Composite Cylinders under Axial Loading // Proceedings of 20th Nordic Seminar on Computational Mechanics. Gothenburg, Sweden, November 2007, pp. 101-104.
9. Bolotin V. V. Statistical Methods in the Nonlinear Theory of Shells // NASA TT F-85 (Translation of a paper presented at a seminar in the Institute of Mechanics of the Academy of Sciences of the USSR, 1957), 1962.
10. Faser W. B., Budiansky B. The Buckling of a Column with Random Initial Deflections // Journal of Applied Mechanics, 36, 1969, pp. 233-240.
11. Amazigo J. C. Buckling under Axial Compression of Long Cylindrical Shells with Random Axisymmetric Imperfections // Quarterly of Applied Mathematics, 26, 1969, pp. 537-566.
12. Tennyson R. C., Muggeridge D. B. Buckling of Laminated Anisotropic Imperfect Circular Cylinders under Axial Compression // Journal of Spacecraft, 10, February 1973, pp. 143-148.
13. Zimmermann R. Buckling Research for Imperfection Tolerant Fiber Composite Structures // Proceedings of Conference on Spacecraft Structures, Materials and Mechanical Testing - Noordwjik, The Netherlands, March 1996, pp. 411-416.
14. Geier B., Klein H., Zimmermann R. Buckling Tests with Axially Compressed Unstiffened Cylindrical Shells Made from CFRP // Proceedings of Buckling of Shell Structures, on Land, in the Sea and in the Air - Lyon, September 1991, pp. 498-507
15. Giavotto V., Poggi C., Castano D., Guzzetti D., Fezzani M. Buckling Behavior of Composite Shells under Combined Loading // Proceedings of 17th European Rotorcraft Forum - Berlin, September 1991, pp. 84-1-84-13.
16. Meyer-Piening H. R., Farshad M., Geier B., Zimmermann R. Buckling Loads of CFRP Composite Cylinders under Combined Axial and Torsion Loading - Experiments and Computations // Composite Structures, 53, 2001, pp. 427-435.
17. Bisagni C., Cordisco P. An Experimental Investigation into the Buckling and Post-buckling of CFRP Shells under Combined Axial and Torsion Loading // Composite Structures, 60, 2003, pp. 391-402.
18. European Standard / Plastics – Determination of tensile properties – Part 4 (EN ISO 527-4:1997)
19. E. Eglītis, K. Kalniņš, O. Ozoliņš, G. Teters, An experimental and numerical study on the dynamic buckling of cylindrical composite shells // Proceedings of International Conference Mechanics of Composite Materials, Riga, Latvia, May 2008, p. 76.
20. ABAQUS Online Documentation: Version 6.8 / Dassault Systèmes, 2008.
21. Release 11.0 Documentation for ANSYS / Ansys, Inc., 2007.
22. Eglitis E., Kalnins K. Benchmarking of FE post-buckling analysis of stiffened composite panels with experimental validation // Proceedings of 4th Conference on Strength, Durability and Stability of Materials and structures - Palanga, September 2007, pp. 32–38.
23. Малмейстер А. К., Тамуж В. П., Тетерс Г. А. Сопротивление полимерных и композитных материалов, 3-е изд., переработанное и дополненное. – Rīga: Zinātne, 1980.

24. Harris L. A., Suer H. S., Skene W. T., Benjamin R. J. The stability of thin-walled unstiffened circular cylinders under axial compression including the effects of internal pressure // Journal of Aeronautical Science, 24, 1957, pp. 587-596.

Edgars Eglītis, Reasearcher, M.sc.ing.
Riga Technical University, Institute of Materials and Structures
Address: Kalku 1, Riga, LV-1658, Latvia
Phone: +371 7089164; Fax: +371 7089254
E-mail: edgars.eglitis@rtu.lv

Kaspars Kalniņš, Leading researcher, Dr. sc.ing.
Riga Technical University, Institute of Materials and Structures
Address: Kalku 1, Riga, LV-1658, Latvia
Phone: +371 7089164; Fax: +371 7089254
E-mail: kaspars.kalnins@sigmanet.lv

Oļģerts Ozoliņš, Researcher, M.sc.ing.
Riga Technical University, Institute of Materials and Structures
Address: Kalku 1, Riga, LV-1658, Latvia
Phone: +371 7089164; Fax: +371 7089254
E-mail: olgerts@bf.rtu.lv

Eglītis E., Kalniņš K., Ozoliņš O. Centriski spiestu kompozīto cilindru noturības eksperimentāls un skaitlisks pētījums
Plānsienu čaulas ir racionālas konstrukcijas, kas ir vieglas un ar augstu nestspēju, taču, atšķirībā no stieņiem un plātnēm, čaulām ir ļoti nestabila pēcnoturības uzvedība, kas sarežģī to projektēšanu un noturības aprēķinus. Centriski spiesta cilindra noturība ir vienkāršs, klasisks čaulas aprēķina uzdevuma piemērs, tomēr iegūt labu sakritību starp aprēķiniem un natūras eksperimentiem joprojām ir grūti. Šī pētījuma ietvaros ir tikuši izgatavoti 18 stikla šķiedras auduma kompozīti cilindri ar sieniņas biezumu 1.1 mm un diametriem 0.3 un 0.5 m, dažādiem augstumiem, kā arī plakani paraugi materiāla elastīgo īpašību noteikšanai. Cilindri tika atkārtoti slogoti pāri noturības robežai, iegūstot slodzes-pārvietojumu līknes un noturības formas attēlus. Salīdzinājumam galīgo elementu programmā ABAQUS tika izveidoti šo cilindru modeļi un veiktas eksperimentu simulācijas, kā arī veikti analītiski kritiskā spēka aprēķini šādiem cilindriem. Pakāpeniski pilnveidojot skaitlisko modeli un papildinot to ar sākotnējām ģeometriskām nepilnībām, ir izdevies iegūt ar eksperimentiem saskanošu rezultātus. Arī eksperimentos novērotās noturības formas atbilst galīgo elementu simulācijās iegūtajām.

Eglītis E., Kalniņš K., Ozoliņš O. Experimental and numerical study on buckling of axially compressed composite cylinders
Thin shells are lightweight, efficient structures that can support very high buckling loads. However, unlike columns and plates, shells usually have a very unstable post-buckling behaviour that strongly influences their buckling characteristics. Axially compressed cylinder may be one of the last classical problems in structural mechanics for which it remains difficult to obtain close agreement between careful experiments and the best predictions from numerical modelling, and therefore much more research is needed on this subject. Within this investigation, 18 glass fibre composite shells with wall thickness of 1.1 mm, 0.3 m and 0.5 m diameters and various lengths have been produced along with flat specimens for determination of elastic properties of the material. The cylinders were repeatedly loaded until post-buckling and load-shortening curves and pictures of buckling mode shapes have been registered. Finite element models of the specimens have been developed in ABAQUS finite element package and non-linear explicit dynamic analyses have been performed for comparison with experimental and analytical results. Gradually improving the finite element model and adding artificial initial imperfections resulted in good agreement between the experimental and numerically obtained critical loads. The buckling modes observed during the experiments are in good agreement with the results of finite element simulations as well.

Эглитис Э., Калниньш К., Озолыньш О. Эксперементальное и численное исследование устойчивости композитных цилиндров под осевым сжатием

Тонкостенные оболочки – это лёгкие, рациональные конструкции, которые способны нести высокие нагрузки. В отличие от стержней и пластин, оболочкам свойственно очень нестабильное пост-критическое поведение и поэтому в инженерных науках проблемы устойчивости оболочек десятилетиями являются актуальными. Центрально сжатый цилиндр является однои из последних задач в строительной механике, для которых до сих пор трудно добиться хорошего совпадения между самыми точными экспериментами и рассчетами, и, следовательно, требуются дополнительные исследования. 18 композитных цилиндров разной длинны, с толщинои стенки 1.1 мм, диаметрами 0.3 м и 0.5 м, а так же плоские образцы для определения механических своиств материала, были подготовлены для данного исследования. Цилиндры подвергались повторному осевому сжатию до пост-критического состояния. При этом записывались диаграммы нагрузки-перемещения и формы потери устоичивости. С помощью программы ABAQUS были разработаны конечно-элементные модели цилиндров и проведен нелинеиный динамический рассчет для сравнения с экспериментальными и аналитическими результатами. Постепенно совершенствуя численную модель, и пополняя её начальними геометрическими несовершенствами удалось получить результаты близкие к эксперементальным.